Influence of synthesis temperature on morphology of SBA-16 mesoporous materials with a three-dimensional pore system

Mohamed A. Ballem, José M. Córdoba and Magnus Odén

Original Publication:

Mohamed A. Ballem, José M. Córdoba and Magnus Odén, Influence of synthesis temperature on morphology of SBA-16 mesoporous materials with a three-dimensional pore system, 2010, Microporous and Mesoporous Materials, (129), 106-111.
http://dx.doi.org/10.1016/j.micromeso.2009.09.004

Influence of synthesis temperature on morphology of SBA-16 mesoporous materials with a three-dimensional pore system

Mohamed Ali Ballem, J.M. Cordoba and Magnus Odén*

Nanostructured Materials, Dept. Physics, Chemistry and Biology, Linköping University, 581 83 Linköping, Sweden

Abstract

Spherical particles of mesoporous silica SBA-16 with cubic *Im3m* structure were synthesized at low pH using Pluronic F127 as template and TEOS as silica source. The diameter of the spherical particles can be controlled in the range of 0.5 – 8 μm by varying synthesis temperature between 1 °C up to 40 °C. A sharp transition from large particle sizes at approximately 20 °C to smaller ones is observed when the temperature is increased. It is suggested that this morphology transition is due to a change in hydrolysis and condensation rate of the silica source and as a result the assembly of F127 micelles will differ. The SBA-16 samples were characterized using powder X-ray diffraction (XRD), scanning electron microscopy (SEM), transmission electron microscopy (TEM) and Nitrogen adsorption techniques.

Keywords: SBA-16; Spherical particles; Synthesis temperature; Morphology; F127

*Corresponding author: magod@ifm.liu.se

1. Introduction

The synthesis of mesoporous materials by a liquid-crystal template mechanism was reported [1, 2] in 1992. The properties of these materials make them attractive for adsorption, catalysis, separation, chemical sensing, optical coating, drug delivery and electronic applications. For practical purposes, the overall morphology of a mesoporous material is a necessary requirement in combination with their internal structure. For instance, in application such as high performance liquid chromatography isometric particles are required [3] and spherical particles are preferably used in chromatography for column packing as irregular particles tend to break down [4].

SBA-16 is a mesoporous material with 3D cubic pore arrangement corresponding to *Im3m* space group. In this body-centered-cubic structure each mesopore is connected with its eight nearest neighbors to form a multidirectional system of mesoporous network [5]. Due to its large cage, high surface area and high thermal stability, this material appears to be one of the best candidates for catalytic support and packing materials for separation. Using F127 as a surfactant is the common way of synthesizing SBA-16 [6, 7]. However, there are also reports on alternative surfactants such as F108 [8], a blend of P123 and F127 [9], and other nonionic surfactants [10].

Several studies have been carried out to understand the formation mechanism of this material, for instance, in the framework of the colloidal phase separation mechanism (CPSM) Yu et al. [11] suggested that, the formation process of mesoporous materials involves three stages: (1) cooperative self-assembly of inorganic/organic composites, (2)

formation of a new crystal-like phase rich in aggregates of block copolymer/silica species, and (3) phase separation of this liquid crystal-like phase from the solution and further growth of solid mesostructures driven by further condensation of silica species. The morphologies of mesoporous materials are developed after step (3) and depend on the competition between the free energy of the mesostructure self-assembly (ΔG) and the colloidal surface free energy (F). Similarly, M. Mesa et al. [12] followed the formation mechanism of SBA-16 from the earliest stage of the reaction until the formation of the particles by a dynamic light scattering technique, and suggested three steps for that: (1) silica coating of the surfactant micelles and decrease of the zeta potential, (2) formation of micron-sized "liquid particles" by aggregation and fusion of the composite colloids (silica coated micelles), and (3) solidification of the "liquid particles" and transformation into the final particles of mesoporous silica.

Synthesis conditions such as temperature, acidity, silica concentration, surfactant type, stirring time, and aging temperature and time affect the morphology evolution of SBA-16. The effect of silica concentration [13, 14], F127 degradation [15], and stirring time [16] on the particle size are documented, while the effect of synthesis temperature on morphology evolution of SBA-16, especially at low temperature, has not yet been reported. Thus, in the present work we show the influence of temperature and how it can be used to tailor the particle size of non agglomerated SBA-16 spheres. The paper also addresses the changes in the lattice parameter, wall thickness, pore size and microporosity properties as a function of temperature, moreover, a mechanism for the formation of these spheres is proposed.

2. Experimental

2.1. Synthesis

Spherical SBA-16 particles have been synthesized using Pluronic F127 ($EO_{106}PO_{70}EO_{106}$, Sigma) as a structured directing agent and TEOS (Tetraethyl orthosilicate, 98 % purity, Aldrich) as a silica source. In a typical synthesis 3.7 g of F127 was dissolved under vigorous stirring into 100 ml (0.2 M) HCl (Hydrochloric acid, 37% concentration, Fluka) at specific temperatures for each sample (1, 10, 15, 20, 25, 30 and 40 °C), the control of these temperatures (± 0.5 °C) was carried out with a cooling/heating device (Julabo F12-ED Refrigerated/Heating Circulator). After three hours 8.56 g of TEOS added to the surfactant solution and kept at the mentioned temperatures under stirring for 20 more hours. The mixture was aged at room temperature for 7 days. The solid product was filtered, washed, and air-dried at room temperature. Calcination was carried out in air by increasing the temperature from room temperature to 560 °C with a heating rate of 1 °C/min, and holding for 5h at 560 °C.

2.2. Characterization

Powder X-ray diffractometry (Philips PW 1729) was used for the determination of crystalline structure, using Cu K_α radiation over $0.5° \leq 2\theta \leq 3$. Scanning electron microscopy (SEM) was performed with a LEO 1550 Gemini Scanning Electron Microscope. The SEM samples were prepared by placing SBA-16 powder on double-sided carbon adhesive tape mounted on the sample holder and then coated with a thin layer of gold in order to minimize charging effects. Transmission electron microscopy (TEM) was

performed with a FEI Tecnai G^2 Microscope operated at 200 kV. The TEM samples were prepared by placing a few drops of SBA-16 powder dispersed in acetone on a carbon grid and allowed to dry for 5 min before TEM analysis. Some of the samples, which have big particles, were crushed by submerging them in liquid nitrogen and mechanical grinding them in a mortar prior to acetone dispersion.

Nitrogen adsorption-desorption measurements were performed at 77 K on a Micromeritics ASAP 2020 Surface area and porosity analyzer. Approximately 0.5 g of SBA-16 was degassed at 573 K for 9h before the measurement. The surface area determination was performed by the Brunauer-Emmett-Teller (BET) method [17] over the relative pressure (P/P_0) range of 0.05 – 0.2, the pore-size distribution was determined using the Broekhoff–de Boer (BdB) method [18] applied to the adsorption branch. Finally the total pore volume was calculated from the amount of adsorbed N_2 at $P/P_0 = 0.99$, and the microporous volume was determined using the *t*-plot method.

3. Results and discussion

Powder X-ray diffractograms of mesoporous SBA-16 samples synthesized at different temperatures are shown in Fig. 1. All the samples synthesized at temperature between 1 and 30° C show the same pattern except for slight shifts in the peak positions toward higher values of 2θ suggesting a decrease in the unit cell (Table 1). The diffractograms show 3 peaks at $2\theta \approx 0.74°$, 1.1° and 1.4°, corresponding to (110), (200) and (211) respectively in the cubic *Im3m* structure. The extracted cubic lattice parameter (a_o) from the diffractograms is summarized in Table 1. a_o decreases more than 1 nm when increasing the temperature from 1 °C (16.7 nm) to 30 °C (15.56 nm). When the synthesis temperature is increased further to 40 °C the presence of only a single reflection indicates the formation of a less ordered structure. At this temperature, the degree of hydration of EO chains decreases and their interaction with the silica species in solution become weaker combined with the increasing rate of the hydrolysis and polymerization of the TEOS source, that lead to formation of amorphous silica.

Figure 2 shows SEM micrographs of SBA-16 morphologies synthesized at various temperatures. The size of the spherical particle is about 8 µm for samples prepared at temperatures between 1 and 20 °C. When increasing the temperature to 25 °C 3 µm particles were obtained, Fig. 2 (e), and for the sample prepared at 30 °C the agglomerated particles are approximately 1 µm, Fig. 2 (f). The particle size versus synthesis temperature is plotted in Fig. 3. It shows plateau between 1 and 20 °C for which the particle size is independent of the synthesis temperature. This plateau offers a robust region for synthesis

of uniform particles, above 20 °C a rather abrupt transition to smaller particles occurs. At temperature between 1 and 20 ^{o}C the average of the particle size is 8 um and it is varying in range between 7.5 to 9 µm, when the temperature is increased above 20 ^{o}C the range of variation is decreased, e.g. it is in the range of 2.8 to 3.2 µm at 25 ^{o}C and 0.9 to 1 µm at 30 ^{o}C.

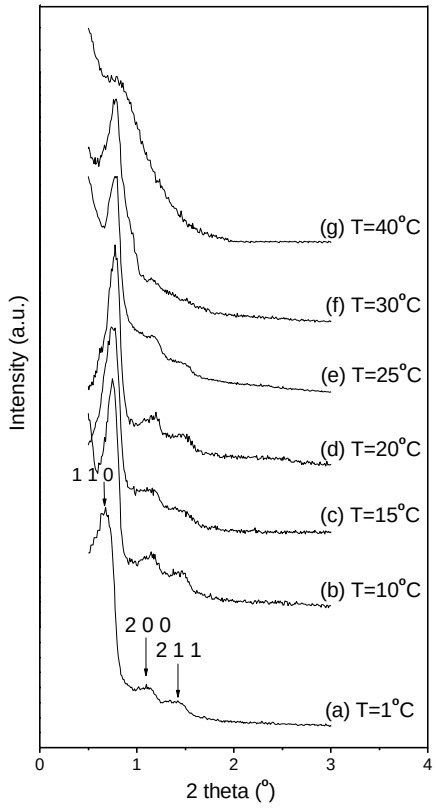

Figure 1 X-ray diffractogram for SBA-16 samples prepared at different temperatures, (a) at T=1, (b) T=10, (c) T=15, (d) T=20, (e) T=25, (f) T=30, (g) T=40 °C.

Table 1 Physical properties of SBA-16 samples synthesized at different temperatures.

Temp. (°C)	d_{110} **(nm)**	a_0 **(nm)**	S_{BET} **(m^2/g)**	***W* (nm)**	D_p **(nm)**	V_{micro} **(cm^3/g)**	V_t **(cm^3/g)**	V_{micro} **/Vt (%)**
1	11.81	16.70	338	10.7	3.8	0.10	0.17	59
10	11.62	16.43	356	10.4	3.8	0.10	0.18	56
15	11.45	16.19	396	10.1	3.9	0.11	0.21	52
20	11.39	16.11	401	10.0	4.0	0.11	0.22	50
25	11.10	15.69	406	9.5	4.1	0.09	0.24	38
30	11.00	15.56	447	9.4	4.1	0.08	0.32	25
40	10.31	14.58	526	8.5	4.1	0.04	0.48	8

d_{110} : the plan spacing at Miller indices 110, a_0 : the cubic lattice parameter ($a_0=\sqrt{2}\ d_{110}$), S_{BET}: BET surface area, W : wall thickness, D_p : pore diameter, V_{micro} : the micropore volume calculated from *t*-plot method, V_t: total pore volume.

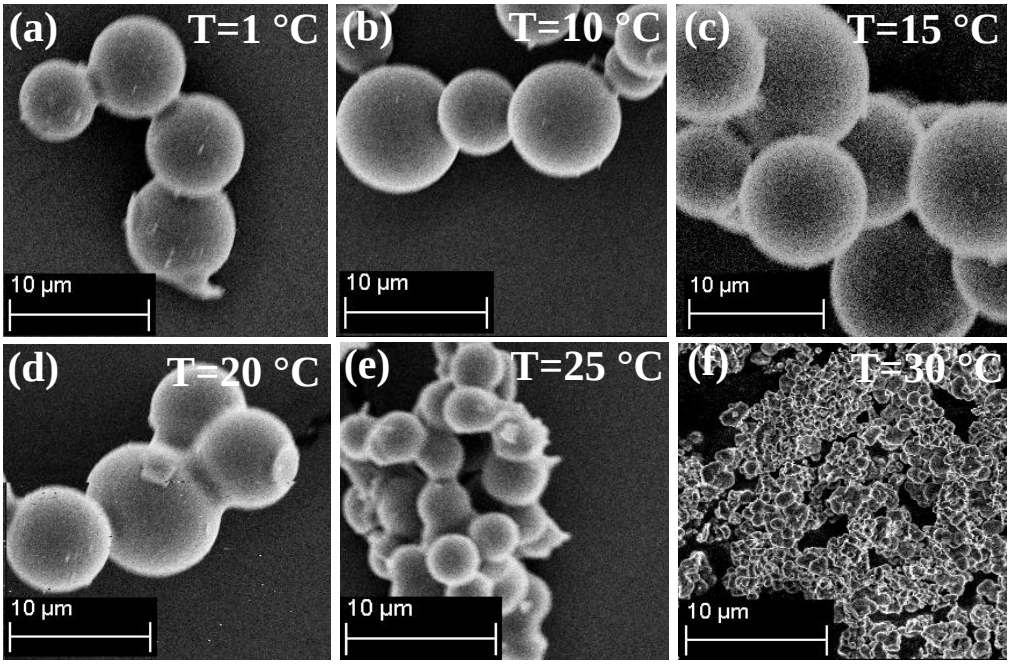

Figure 2 Scanning electron micrographs of SBA-16 morphologies synthesized at different temperatures: (a) at T=1, (b) T=10, (c) T=15, (d) T=20, (e) T=25, (f) T=30 °C.

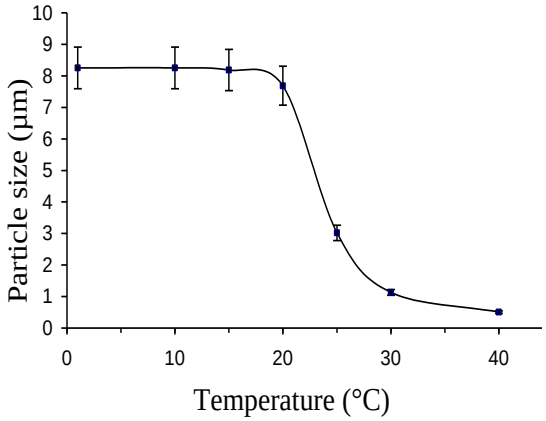

Figure 3 The relation between the synthesis temperature and the diameter of SBA-16 sphers.

Figure 4 (a) shows a TEM micrograph of particles prepared at 40 °C, the size of the particles about 0.5 µm. Figure 4 (b) shows the mixed nature of this sample with ordered structure in some areas and the rest being amorphous, which is consistent with the XRD results. Figure 5 (a) shows pieces of particles prepared at 1 °C after grinding them mechanically in a mortar and pestle treating them with liquid nitrogen and then, (b) TEM observation for one of the pieces at (a) is confirmed that each spherical particle is a perfect single crystal with porous arranged in a cubic structure. The obtained ordered pores here is distinctly different from the observations made by M. Mesa et al. [15] who reported that at temperatures of 40 °C or lower, the gel-like particles with poorly organized mesostructure are difficult to transform into well-organized materials. The synthesis parameters we used differ compared to their study. Mesa et al. used a cationic co-surfactant, different molar ratio of the other chemicals, and different dwell times in the different synthesis steps. Our

study and others [6, 12, 13] show the importance of carful tuning of the synthesis parameters in order to obtain high quality SBA-16 when working at low temperatures.

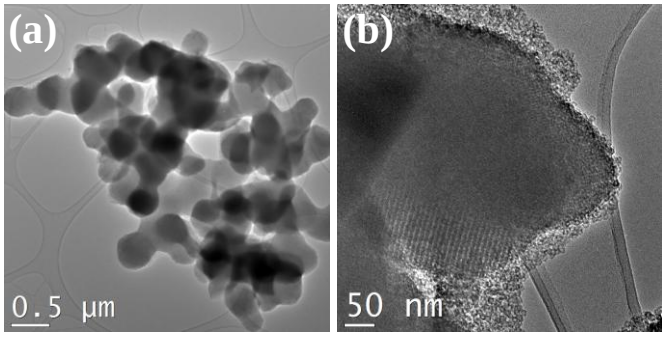

Figure 4 Transmission electron micrographs of (a) SBA-16 particles prepared at temperature 40 °C, and (b) their pore structure.

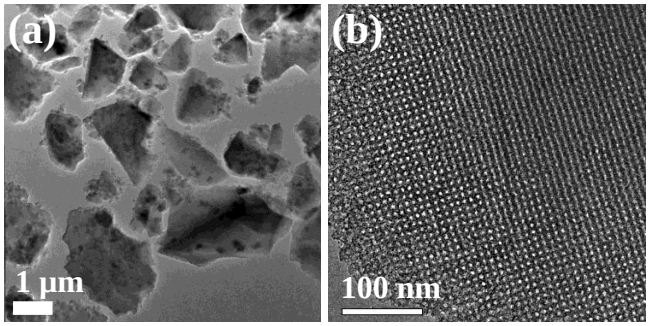

Figure 5 Transmission electron micrographs of (a) a fractured particles prepared at 1 °C, and (b) their pore structure.

A formation mechanism of the spherical SBA-16 is proposed in Fig. 6, and it is based on the colloidal phase separation mechanism (CPSM) [11]. When the surfactant $EO_{106}PO_{70}EO_{106}$ is added to the acidic solution micelles will start to form, Fig. 6 Step 1. The EO chains are more hydrophilic at low temperature ($T \leq 20$ °C), so the micelles have longer EO chains Fig. 6 (a) step 1, while at higher temperatures ($T > 20$ °C, Fig 6 (b)) the EO chains become more hydrophobic and withdraw to the PO core leading to an increase in micelle core size and a decrease in the EO chain lengths [13].

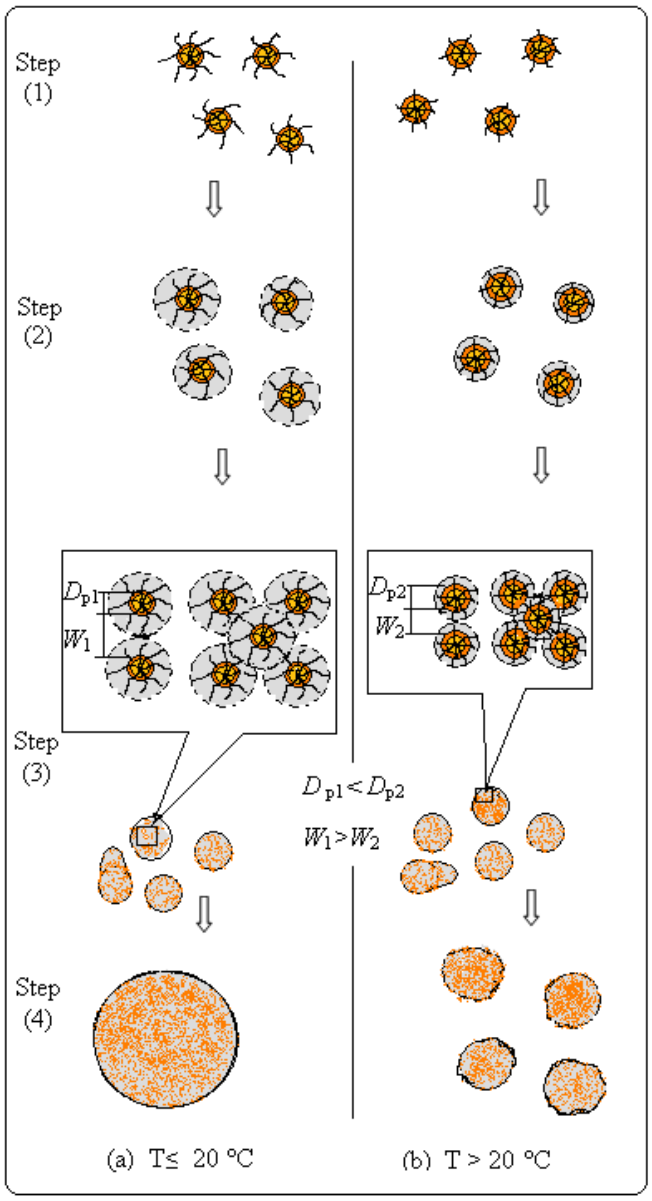

Figure 6 Schematic drawing of the formation steps of SBA-16 spheres, (a) at synthesis temperature ≤ 20 °C and (b) at synthesis temperature > 20 °C.

After adding the silica the EO chains will attract the cationic silica oligomer and catalyze silica polymerization on the surface of the micelles forming silicated micelles. In acidic media (pH ≤ 2) surfactant/silica interaction occurs through an $(S^0H^+)(X^-I^+)$ pathway (S^0H^+ being the surfactant hydrogen-bonded to a hydronium ion, X^- the chloride ion, and

the protonated silica) [19], which gives rise to step 2 in Fig. 6. The interaction between EO and silica cations will be stronger at low temperature [7] so the micelles will have a thicker silica coating compared to higher synthesis temperature, which explains the larger lattice parameter seen at low temperature. The coated micelles assemble and form liquid particles of SBA-16 with cubic structure (Fig. 6 step 3). According to CPSM this interconnection between the surfactant/silica aggregates occurs due to further condensation of silica species. From a colloidal point of view, the coated micelles will behave as classical colloidal particles, which mean that they will follow the rules of colloidal solutions and finally they will aggregate and fuse together to form the liquid particles (Fig. 6 step 3), which will transform into the final particles (Fig. 6 step 4), the details of this step have been discussed extensively by M. Mesa et al. [12] using the DLVO (Derjaguin, Landau, Verwey and Overbeek) theory.

We propose that different particle sizes at different temperatures originate after the phase separation step where the competition between (ΔG) and (F) will determine the final morphology of the mesoporous material. At low temperature the silica condensation is low [19, 20, 21], which results in a slow phase separation rate. Thus, the morphology is controlled by surface energy effects (F), so particles with small radius will grow larger in order to minimize the surface area (Fig. 6 (a) step 4). However, at higher temperatures and because of a high hydrolysis and condensation rate of the silica source [7] the phase separation occurs earlier and ΔG dominates the particle growth, i.e. the obtained particles are not as smooth as the ones produced at low temperatures (Fig. 6 (b) step 4) . An additional effect of the increased rate of silica polymerization is the increased viscosity of

the medium which slows down the particle growth. Hence, allowing for many particles to nucleate instead [22], Fig. 6 step 4.

The isotherms and pore size distributions (insets) for SBA-16 samples synthesized at temperature between 1 °C and 40 °C are shown in Fig. 7. The nitrogen sorption isotherms exhibit type IV shapes according to the IUPAC classification [23]. For pore size in the range of 3.6 to 3.8 nm previous studies have shown an absence of a hysteresis loop [24], which we also see for samples synthesized at low temperatures (1 and 10 °C). The sample prepared at 40 °C shows a slightly different isotherm as expected from its different pore structure. The average pore size (D_p) increases from 3.8 nm (1 °C) to 4.1 nm (40 °C), which is expected due to less hydrophilic EO-chains which results in larger micelle cores at higher temperatures. For similar reasons, the volume fraction micropores to the total pore volume of SBA-16 materials is decreasing from 59 % (1 °C) to 8 % (40 °C). The structural parameters extracted at different temperature are summarized in table 1.

When increasing the temperature from 1 to 40 °C the BET surface increases because at high temperature the particles have higher pore volume and a larger external surface area due to their small sizes. The wall thickness, which is calculated by $W= \sqrt{3}a_0/2-D_p$ [25], decreases when the temperature increases due to the weak interaction between the silica and EO parts at high temperature [7], or in other words the thickness of silica coat of F127 micelles is thinner at high temperature as it is shown in Fig. 6 step 2 and 3.

Controlling the particle size is an important parameter especially on the stationary phases for separation application. The extreme thickness of the wall shown here gives a

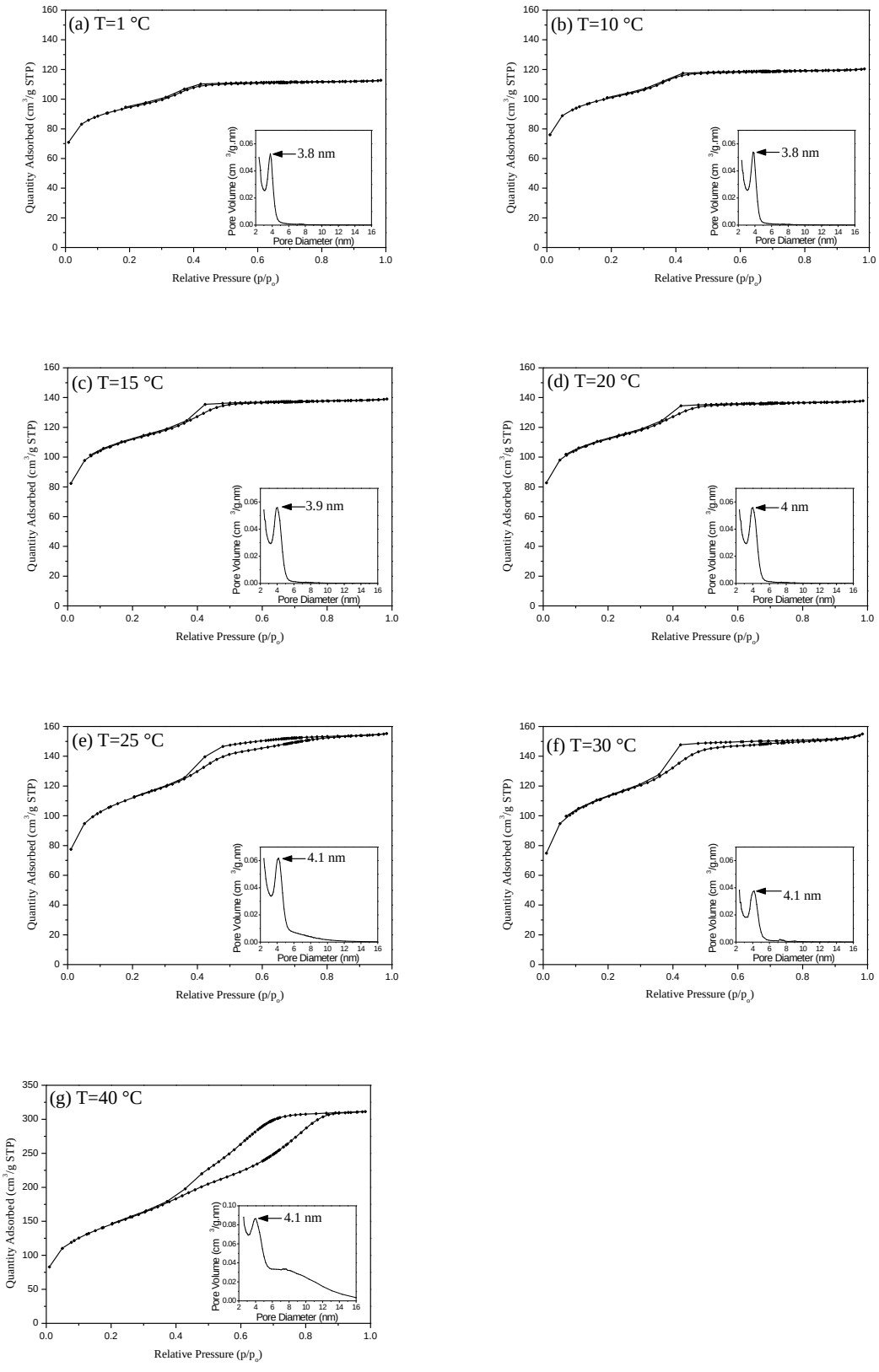

Figure 7 Nitrogen adsorption–desorption isotherms and pore size distributions (insets) for SBA-16 materials synthesized at different temperatures: (a) at T= 1, (b) T=10, (c) T= 15, (d) T= 20, (e) T= 25, (f) T= 30 and (g) T= 40 °C.

high thermal and hydrothermal stability, which is useful if these materials are used as templates for synthesis of nanoparticles.

4. Conclusion

In the present work, we have shown that the size of spherical particles of SBA-16 mesoporous materials can be simply tailored in the range of 0.5–8 μm by varying synthesis temperature. These materials can be obtained in acidic medium (0.2M HCl) by using of F127 and TEOS with molar ratio 0.007. A formation mechanism of these spheres is proposed, which explains the distinct sizes obtained, moreover the changes in the structural properties of SBA-16 during the variation of the synthesis temperature is presented.

References

[1] J.S. Beck, J.C. Vartuli, W.J. Roth, M.E. Leonowicz, C.T. Kresge, K.D. Schmitt, C.T.W. Chu, D.H. Olson, E.W. Sheppard, S.B. McCullen, J.B. Higgins, J.L. Schlenker, J. Am. Chem. Soc. 114 (1992) 10834.

[2] C.T. Kresge, M.E. Leonowicz, W.J. Roth, J.C. Vartuli, J.S. Beck, Nature 359 (1992) 710.

[3] C. Boissiere, M. Kummel, M. Persin, A. Larbot and E. Prouzet, Adv. Funct. Mater. 11 (2001) 129.

[4] H.B.S. Chan, P.M. Budd, T.D. Naylor, J. Mater. Chem. 11 (2001) 951.

[5] Y. Sakamoto, M. Kaneda, O. Terasaki, D.Y. Zhao, J.M. Kim, G. Stucky, H.J. Shin, R. Ryoo, Nature 408 (2000) 449.

[6] D. Zhao, Q. Huo, J. Feng, B.F. Chmelka, G.D. Stucky, J. Am. Chem. Soc. 120 (1998) 6024.

[7] P. van der Voort, M. Benjelloun, E.F. Vansant, J. Phys. Chem. B 106 (2002) 9027.

[8] P. Kipkemboi, A. Fogden, V. Alfredsson, K. Flodström, Langmuir 17 (2001) 5398.

[9] T.W. Kim, R. Ryoo, M. Kruk, K. P. Gierszal, M. Jaroniec, S. Kamiya, O. Terasaki, J. Phys. Chem. B, 108 (2004) 11480.

[10] L. Wang, J. Fan, B. Tian, H. Yang, Ch. Yu, B. Tu, D. Zhao, Micropor. Mesopor. Mater. 67 (2004) 135.

[11] C. Yu, J. Fan, B. Tian, D. Zhao, Chem. Mater. 16 (2004) 889.

[12] M. Mesa, L. Sierra, J.L. Guth, Micropor. Mesopor. Mater. 112 (2008) 338.

[13] C.F. Cheng, Y.C. Lin, H.H. Cheng, Y.C. Chen, Chem. Phys. Lett. 382 (2003) 496.

[14] W.J.J. Stevens, M. Mertens, S. Mullens, I. Thijs, G.V. Tendeloo, P. Cool, E.F. Vansant, Micropor. Mesopor. Mater. 93 (2006) 119.

[15] M. Mesa, L. Sierra, J. Patarin, J.L. Guth, Solid State Sci. 7 (2005) 990.

[16] Y.K. Hwang, J.S. Chang, Y.U. Kwon, S.E. Park, Micropor. Mesopor. Mater. 68 (2004) 21.

[17] S. Brunauer, P. H. Emmett, E. Teller, J. Am. Chem. Soc. 60 (1938) 309.

[18] W.W. Lukens, P. Schmidt-Winkel, D.Y. Zhao, J.L. Feng, G.D. Stucky, Langmuir, 15 (1999) 5403.

[19] Q. Huo, D.I. Margolese, U. Ciesla, D.G. Demuth, P. Feng, T.E. Gier, P. Sieger, A. Firouzi, B.F. Chmelka, F. Schüth, G.D. Stucky, Chem. Mater. 6 (1994) 1176.

[20] B.C. Chen, M.C. Chao, H.P. Lin, C.Y. Mou, Micropor. Mesopor. Mater. 81 (2005) 241.

[21] N. Brodie-Linder, G. Dosseh, C. Alba-Simonesco, F. Audonnet, M. Imperor-Clerc, Mater. Chem. Phys. 108 (2008) 73.

[22] D. J. Shaw, Introduction to Colloid and Surface Chemistry, 4th ed., Reed Educational and Professional Publishing Ltd, UK, 1991.

[23] K.S.W. Sing, D.H. Everett, R.A.W. Haul, L. Moscou, R.A. Pierotti, J. Rouquerol, T. Siemieniewska, Pure and Applied Chemistry, 57 (1985) 603.

[24] S. Inoue, Y. Hanzawa, K. Kaneko, Langmuir, 14 (1998) 3079.

[25] P.I. Ravikovitch, A.V. Neimark, Langmuir 18 (2002) 1550.